JCI The Journal of Clinical Investigation

Osteoprotegerin inhibits prostate cancer–induced osteoclastogenesis and prevents prostate tumor growth in the bone

Jian Zhang, … , John Westman, Evan T. Keller

J Clin Invest. 2001;107(10):1235-1244. https://doi.org/10.1172/JCI11685.

Article

Prostate cancer (CaP) forms osteoblastic skeletal metastases with an underlying osteoclastic component. However, the importance of osteoclastogenesis in the development of CaP skeletal lesions is unknown. In the present study, we demonstrate that CaP cells directly induce osteoclastogenesis from osteoclast precursors in the absence of underlying stroma in vitro. CaP cells produced a soluble form of receptor activator of NF-κB ligand (RANKL), which accounted for the CaP-mediated osteoclastogenesis. To evaluate for the importance of osteoclastogenesis on CaP tumor development in vivo, CaP cells were injected both intratibially and subcutaneously in the same mice, followed by administration of the decoy receptor for RANKL, osteoprotegerin (OPG). OPG completely prevented the establishment of mixed osteolytic/osteoblastic tibial tumors, as were observed in vehicle-treated animals, but it had no effect on subcutaneous tumor growth. Consistent with the role of osteoclasts in tumor development, osteoclast numbers were elevated at the bone/tumor interface in the vehicle-treated mice compared with the normal values in the OPG-treated mice. Furthermore, OPG had no effect on CaP cell viability, proliferation, or basal apoptotic rate in vitro. These results emphasize the important role that osteoclast activity plays in the establishment of CaP skeletal metastases, including those with an osteoblastic component.

Osteoprotegerin inhibits prostate cancer–induced osteoclastogenesis and prevents prostate tumor growth in the bone

See related Commentary on pages 1219–1220.

Jian Zhang,[1] Jinlu Dai,[2] Yinghua Qi,[3] Din-Lii Lin,[2] Peter Smith,[2] Chris Strayhorn,[4] Atsushi Mizokami,[5] Zheng Fu,[6] John Westman,[4] and Evan T. Keller[1,2,6,7]

[1]Department of Pathology, and
[2]Unit for Laboratory Animal Medicine, School of Medicine, University of Michigan, Ann Arbor, Michigan, USA
[3]Laboratory of Cellular and Molecular Biology, Department of Internal Medicine, Tianjin 3rd Municipal Hospital, Tianjin, China
[4]Department of Pathology, School of Dentistry, University of Michigan, Ann Arbor, Michigan, USA
[5]Department of Urology, School of Medicine, Kanazawa University, Kanazawa, Japan
[6]Program in Immunology, and
[7]Connective Tissue Oncology Program, School of Medicine, University of Michigan, Ann Arbor, Michigan, USA

Address correspondence to: Evan T. Keller, Room 5304 CCGCB Box 0940, 1500 E. Medical Center Drive, Ann Arbor, Michigan 48109-0940, USA. Phone: (734) 615-0280; Fax: (734) 936-9220; E-mail: etkeller@umich.edu.

Received for publication October 31, 2000, and accepted in revised form March 27, 2001.

Prostate cancer (CaP) forms osteoblastic skeletal metastases with an underlying osteoclastic component. However, the importance of osteoclastogenesis in the development of CaP skeletal lesions is unknown. In the present study, we demonstrate that CaP cells directly induce osteoclastogenesis from osteoclast precursors in the absence of underlying stroma in vitro. CaP cells produced a soluble form of receptor activator of NF-κB ligand (RANKL), which accounted for the CaP-mediated osteoclastogenesis. To evaluate for the importance of osteoclastogenesis on CaP tumor development in vivo, CaP cells were injected both intratibially and subcutaneously in the same mice, followed by administration of the decoy receptor for RANKL, osteoprotegerin (OPG). OPG completely prevented the establishment of mixed osteolytic/osteoblastic tibial tumors, as were observed in vehicle-treated animals, but it had no effect on subcutaneous tumor growth. Consistent with the role of osteoclasts in tumor development, osteoclast numbers were elevated at the bone/tumor interface in the vehicle-treated mice compared with the normal values in the OPG-treated mice. Furthermore, OPG had no effect on CaP cell viability, proliferation, or basal apoptotic rate in vitro. These results emphasize the important role that osteoclast activity plays in the establishment of CaP skeletal metastases, including those with an osteoblastic component.

J. Clin. Invest. **107**:1235–1244 (2001).

Introduction

Prostate cancer is the most frequently diagnosed cancer in men and the second leading cause of cancer death among men in the US. The most common site of prostate cancer metastasis is the bone, with up to 84% of patients demonstrating skeletal metastases (1). While initially thought to be primarily osteoblastic, it is now recognized that prostate cancer skeletal metastases have an extensive bone resorptive component (2, 3) that is caused primarily by osteoclasts (4). This accounts, in part, for the ability of bisphosphonates, which are anti-osteoclastogenic agents, to diminish osteolysis, decrease pain, and improve mobility in patients with prostate cancer skeletal metastasis (5). However, the mechanisms through which prostate cancer skeletal metastases induce osteolytic lesions are not defined.

The presence of an osteolytic component in prostate cancer skeletal metastases suggests that osteoclastogenesis may play a role in the establishment of these lesions. Recently, the discovery and characterization of a novel cytokine system — the TNF family member, receptor activator of NF-κB ligand (RANKL, also called OPGL, TRANCE, and ODF); its receptor, receptor activator of NF-κB (RANK, also called ODAR); and its decoy receptor, osteoprotegerin (OPG, also called OCIF and TR1) — has established a common mechanism through which osteoclastogenesis is regulated in normal bone (reviewed in ref. 6). RANKL, a transmembrane molecule located on bone marrow stromal cells and osteoblasts, binds to RANK, which is located on the surface of osteoclast precursors. This ligand-receptor interaction activates NF-κB, which stimulates differentiation of osteoclast precursors to osteoclasts. OPG, also produced by osteoblasts/stromal cells, binds to RANKL, sequestering it from binding to RANK, which results in inhibition of osteoclastogenesis. The requirement for RANKL to induce osteoclastogenesis suggests that it may mediate the osteolytic component of prostate cancer skeletal lesions. However, it is currently unknown if prostate cancer uses the

RANKL:RANK axis to induce osteolysis. Furthermore, OPG has been shown to inhibit primary bone sarcoma–induced osteolysis and tumor-induced bone pain, but not tumor burden in mice (7). However, the role of OPG on tumors metastatic to bone or epithelial tumors remains undetermined. Accordingly, in the current study, we investigated the mechanism through which prostate cancer induces osteoclastogenesis and determined if OPG could inhibit establishment of prostate tumor in murine bone.

Methods

Animals. Eight-week-old male SCID and C57BL/6 mice (Charles River, Wilmington, Massachusetts, USA) were housed under pathogen-free conditions in accordance with the NIH guidelines using an animal protocol approved by the University of Michigan Animal Care and Use Committee.

Cell lines. The human prostate cell line LNCaP (American Type Tissue Collection, Manassas, Virginia, USA) derived from an aspirate of a subcutaneous supraclavicular lymph node prostate cancer metastases, was maintained in RPMI-1640 supplemented with 10% FBS, 100 U/l penicillin G, 100 μg/ml streptomycin, and 2 mM L-glutamine. LNCaP cells induce very low levels of blastic activity when implanted into bone and do not readily metastasize (8). C4-2B cells (UroCor Inc., Oklahoma City, Oklahoma, USA) are derived from LNCaP cells after several passages through nude mice and aggressive tumors that metastasize to bone (8, 9). The C4-2B cells were maintained in T medium, which consisted of 80% DMEM (Life Technologies Inc., Grand Island, New York, USA), 20% F12K (Irving Scientific, Santa Ana, California, USA), 3 g/l $NaHCO_3$, 100 U/l penicillin G, 100 μg/ml streptomycin, 5 μg/ml insulin, 13.6 pg/ml triiodothyronine, 5 μg/ml apo-transferrin, 0.25 μg/ml biotin, 25 μg/ml adenine, and were supplemented with 10% FBS. The human osteogenic sarcoma cell line SaOS (American Type Tissue Collection), was maintained in DMEM supplemented with 10% FBS, 100 U/l penicillin G, 100 μg/ml streptomycin, and 2 mM L-glutamine. Murine monocyte/macrophage-like cell line, RAW 264.7, commonly used as an osteoclast precursor cell line (American Type Tissue Collection), was maintained in RPMI-1640 supplemented with 10% FBS, 100 U/l penicillin G, 100 μg/ml streptomycin, and 2 mM L-glutamine.

Tumor implant. Single-cell suspensions (3×10^5 cells) of C4-2B cells in T media were injected into the right tibia of 8-week-old male SCID mice (n = 30) as described previously (10). Briefly, mice were anesthetized (135 mg ketamine, 15 mg xylazine/kg body weight), the knee was flexed, and a 26-g, 3/8-inch needle was inserted into the proximal end of right tibia followed by injection of 20 μl of the cell suspension.

Subcutaneous tumors. At the same time as intratibial injection, C4-2B cells were resuspended in T media plus 10% FBS. Two million cells were mixed 1:1 with Matrigel (Collaborative Biomedical Products, Bedford, Massachusetts, USA), and then injected in the flank at 100 μl/site using a 23-g needle. Subcutaneous tumor growth was monitored by palpation, and two perpendicular axes were measured; the tumor volume was calculated using the formula as described previously (11): volume = length × width^2/2.

Treatment. At the time of injection, mice were randomized to receive either injections (through tail vein) of vehicle (1% BSA in 1× PBS) (n = 10) or recombinant mouse OPG/Fc chimera (R&D Systems Inc., Minneapolis, Minnesota, USA) at 2 mg/kg body weight (n = 10) twice a week and continued for 4 weeks. Tumors were allowed to grow for 16 weeks, and at the end of week 16, all animals were sacrificed. One animal in the OPG treatment group died 1 day after the tumor was implanted. To evaluate histology at a 4-week time point, we performed the same protocol with another five vehicle-treated and five OPG-treated mice. Before sacrifice, the animals were anaesthetized, and magnified flat radiographs were taken with a Faxitron (Faxitron X-Ray Corp., Wheeling, Illinois, USA). At sacrifice, all of the major organs and lumbar vertebrae were harvested for histological analysis.

Histopathology and bone histomorphometry. Histopathology was performed as we have described previously (12). Briefly, bone specimens were fixed in 10% formalin for 24 hours, then decalcified using 12% EDTA for 72 hours. The specimens were then paraffin embedded, sectioned (5 μM), and stained with hematoxylin and eosin to assess histology or stained with tartrate-resistant acid phosphatase (TRAP) to identify osteoclasts. To perform TRAP staining, nonstained sections were deparaffinized and rehydrated, then stained for TRAP (Acid Phosphatase Kit 387-A; Sigma Diagnostics, St. Louis, Missouri, USA) as directed by the manufacturer, with minor modification. Briefly, the specimens were fixed for 30 seconds and then stained with acid phosphatase and tartrate solution for 1 hour at 37°C, followed by counterstaining with hematoxylin solution. Osteoclasts were determined as TRAP-positive staining multinuclear (>3 nuclei) cells using light microscopy. Histomorphometric analysis was performed on a BIOQUANT system (BIOQUANT-R&M Biometrics Inc., Nashville, Tennessee, USA). The osteoclast perimeter (osteoclast number per millimeter of bone) in vehicle-treated animals compared with normal bone surface in the OPG-treated animals was quantified, without knowledge of treatment group, by examination at ×200. For routine histopathology, soft tissues were preserved in 10% formalin, embedded in paraffin, sectioned (5 μM), and stained with hematoxylin and eosin.

Prostate-specific antigen immunohistochemistry. Nonstained sections were deparaffinized and rehydrated then stained for prostate-specific antigen (PSA) with anti-human PSA Ab using standard immunohistochemistry techniques. Human prostate cancer tissue and normal prostate tissue were used as a positive control and a negative control, respectively.

Obtaining conditioned media. Conditioned media (CM) was obtained from LNCaP or C4-2B cells by plating 5×10^6 cells in 10-cm tissue culture dishes for 12 hours in T media with 10% FBS. The media was then changed to 10 ml of RPMI plus 0.5% FBS, and supernatants were collected 24 hours later. To normalize for differences in cell density due to proliferation during the culture period, cells from each plate were collected, and total DNA content/plate was determined (spectrophotometric absorbance at 260 nm). CM was then normalized for DNA content between samples by adding RPMI.

Assessment of ability of prostate cancer cells to induce osteoclastogenesis in the presence of osteoblast/stromal cells in vitro. To establish cocultures, single cell suspensions (10^5 cells/well) of LNCaP or C4-2B cells were plated on sterile glass coverslips in 24-well plates in RPMI or T media plus 10% FBS. Cells were grown for 12 hours, then media was changed to RPMI plus 0.5% FBS. Then, all wells were overlaid with single-cell suspension of murine bone marrow cells (10^6 cells in 1 ml media) from six healthy C57BL mice. In addition to the cocultures, CM at different concentrations was added directly to murine bone marrow cells in the absence of prostate cancer cells. Vitamin D was not added to either the cocultures or the CM cultures. Recombinant OPG (R&D Systems Inc.) in indicated concentrations, vehicle (1% BSA in 1× PBS), or M-CSF (1 ng/ml) (Sigma Diagnostics) was added to the cultures. The cultures were maintained for 9 days with replacement of half the medium (including the different concentrations of CM with indicated treatments) every 3 days. Samples were evaluated in quadruplicates. Osteoclast-like cells were identified as TRAP-positive multinucleated (>3 nuclei) cells. Results were reported as the number of osteoclast-like cells per coverslip.

Assessment of ability of prostate cancer cells to induce osteoclastogenesis in the absence of osteoblast/stromal cells in vitro. Single-cell suspensions (10^5 cells/well) of RAW 264.7 cells were plated on sterile glass coverslips in 24-well plates in RPMI plus 10% FBS. Cells were grown for 12 hours then the media was changed to RPMI plus 0.5% FBS. CM (25%; CM volume/total culture volume) from C4-2B cells was added to the RAW 264.7 cell cultures. Additionally, recombinant human RANKL (10 ng/ml; PeproTech Inc., Rocky Hill, New Jersey, USA), recombinant OPG (R&D Systems Inc.) as indicated, or vehicle (1% BSA in 1× PBS) was added. These cultures did not contain vitamin D. The cultures were maintained for 7 days with replacement of half the medium (including 25% CM with indicated treatment) at day 3. Samples were evaluated in quadruplicate. Osteoclast-like cells were identified as TRAP-positive multinucleated (>3 nuclei) cells. Results were reported as the number of osteoclast-like cells per coverslip.

RANKL mRNA expression. Total RNA from LNCaP and C4-2B cells was collected (Trizol reagent; Life Technologies Inc.), then subjected to PCR for detection of RANKL mRNA. PCR primers used for detection of RANKL consisted of sense, 5′-GCTTGAAGCTCAGCCTTTTGCTCAT-3′, and antisense, 5′-GGGGTTGGAGACCTCGATGCTGATT-3′, resulting in a PCR product of 412 bp (primer sequence kindly provided by J. Brown, University of Washington, Seattle, Washington, USA). The human osteoblastic-like/osteosarcoma SaOS cell line was used as a positive control for OPGL expression. RT-PCR was performed with 1 μg of total RNA using the Access RT-PCR system (Promega Corp., Madison, Wisconsin, USA), as directed by the manufacturer, in a thermal cycler (GeneAmp PCR system 9700; Perkin-Elmer Applied Biosystems, Foster City, California, USA) under the following conditions: first-strand cDNA was synthesized at 48°C for 45 minutes; then denatured at 94°C for 2 minutes for the first cycle and at 15 seconds for additional 35 cycles; annealing was performed at 55°C for 30 seconds; and extension at 72°C for 60 seconds. Final extension was at 72°C for 5 minutes. The PCR products were subjected to electrophoresis on a 1.5% agarose gel, stained with ethidium bromide.

Western blot analysis. To evaluate for RANKL in the prostate cancer cell supernatant, CM collected from LNCaP and C4-2B cell cultures were concentrated 100-fold using a 10-kDa cut-off Microcon centrifugal filter devices (Amicon Inc., Beverly, Massachusetts, USA). To evaluate for RANKL expression in the prostate cancer cells, confluent LNCaP and C4-2B cells were washed twice with PBS and then lysed in RIPA buffer (1× PBS, 1% Nonidet P-40, 0.5% sodium deoxycholate, 0.1% SDS) with 100 ng/ml PMSF. Proteins (50 μg/lane) from the concentrated CM and cell lysates were applied to SDS-PAGE followed by Western blot analysis with rabbit anti-human soluble RANKL polyclonal Ab (PeproTech Inc.). The Ab binding was revealed using an HRP-conjugated anti-rabbit IgG (Amersham Pharmacia Biotech, Piscataway, New Jersey, USA) and enhanced chemiluminescence (ECL) blot detection system (Amersham Pharmacia Biotech).

Cell viability. C4-2B cells were plated at 2×10^6/plate in 60-mm plates in triplicate with T media. After 12 hours of culture, media was changed to RPMI plus 0.5% FBS, and recombinant OPG (R&D Systems Inc.) was added at different concentrations (0–100 ng). Subsequently, cells were harvested at 24 hours and viability was examined by trypan blue exclusion.

Cell proliferation. Cell proliferation was measured using the CellTiter 96 AQ nonradioactive cell proliferation assay (Promega Corp.). Briefly, C4-2B cells in T media were added to the wells of a 96-well plate at 5,000/well in triplicates. After 12 hours of culture, the media was changed to RPMI plus 0.5% FBS and a different concentration (0–100 ng) of recombinant OPG (R&D Systems Inc.) was added. Cells were allowed to grow for 24 hours, then 20 μl/well of combined MTS/PMS solution was added. After incubation of 1 hour at 37°C in a humidified 5% CO_2 atmosphere, the absorbance at 490 nm was recorded by using an ELISA plate reader.

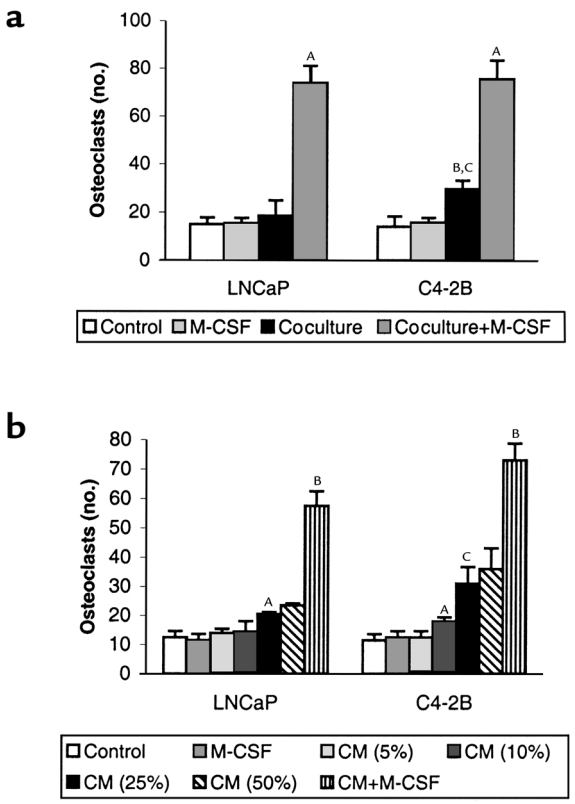

Figure 1
OPG inhibits LNCaP and C4-2B cell–induced osteoclastogenesis of osteoblast/stromal cells in vitro. (**a**) LNCaP or C4-2B cells were directly cocultured with murine bone marrow cells for 9 days in the presence or absence of M-CSF (1 ng/ml). Osteoclast-like cells were identified as TRAP-positive multinucleated (>3 nuclei) cells. $^{A}P < 0.001$ compared with its respective control culture (without adding CaP cells) or coculture; $^{B}P < 0.01$ compared with its respective control culture; $^{C}P < 0.01$ compared with its LNCaP cells. (**b**) Conditioned media (CM) from LNCaP and C4-2B cells was collected after 24 hours of culture, then the indicated concentrations of CM (vol/vol) was added to murine bone marrow cells and cultured for 9 days. Osteoclast-like cells were identified as TRAP-positive multinucleated (>3 nuclei) cells. $^{A}P < 0.001$ compared with respective control culture (without adding CM); $^{B}P < 0.001$ compared with each cell line's respective control culture or coculture; $^{C}P < 0.01$ compared with its LNCaP cells. (**c**) CM (25% vol/vol) from LNCaP and C4-2B cells were collected after 24 hours of culture, then added to murine bone marrow cells with different dose of recombinant mouse OPG (1–1000 ng/ml) as indicated and cultured for 9 days. Osteoclast-like cells were identified as TRAP-positive multinucleated (>3 nuclei) cells. $^{A}P < 0.001$ compared with its control culture; $^{B}P < 0.01$ compared with its respective vehicle-treated CM cultures; $^{C}P < 0.001$ compared with its respective vehicle-treated CM cultures. All in vitro cultures were evaluated in quadruplicate. Results were reported as the mean (± SD) number of osteoclast-like cells per coverslip. Data were analyzed using ANOVA and Fisher's least-significant difference for post hoc analysis.

Cell apoptosis. C4-2B cells were plated at 10^6/well in 12-well plates in triplicate with T media. After 12 hours of culture, media was changed to RPMI plus 0.5% FBS and immediately a different concentration (0–100ng) of recombinant OPG (R&D Systems Inc.) was added. Subsequently, cells were harvested at 24 hours, and apoptosis was assessed by flow cytometry using Annexin V-FITC detection Kit (PharMingen, San Diego, California, USA) following the manufacturer's protocol.

Data analysis. Fisher's exact test was used to determine if there was a difference in the incidence of tumor development between groups. ANOVA was used for the in vitro culture system to evaluate differences in prostate cancer cell–induced osteoclastogenesis. Fisher's least-significant difference was used for post hoc analysis. Student's *t* test was used for bivariate comparisons. P values less than or equal to 0.05 were considered to be statistically significant.

Results

The mechanism through which prostate cancer induces osteolysis at its skeletal metastatic site has not been defined. To test whether prostate cancer cells induce osteoclastogenesis in vitro, LNCaP and C4-2B cells were directly cocultured with murine bone marrow cells for 9 days in 1,25 $(OH)_2$ vitamin D_3–free (VitD-free) media. LNCaP and C4-2B cells induced approximately 30% and 90% increase of osteoclasts compared with marrow control cultures without prostate cancer cells, respectively (Figure 1a). The addition of M-CSF, a strong costimulator of osteoclastogenesis, synergistically enhanced the prostate cancer cell–induced osteoclastogenesis (Figure 1a). A variety of soluble factors such as IL-6, PTHrP, and soluble RANKL may act to induce osteoclastogenesis (13). Thus, to determine if the prostate cancer cells induced osteoclastogenesis through a soluble factor, we tested the ability of CM from LNCaP and C4-2B cell cultures to induce osteoclastogenesis in vitro. CM was added to murine bone marrow cells and culture was maintained for 9 days. The CM induced osteoclastogenesis in a dose-responsive fashion (Figure 1b). C4-2B cells induced approximately 80% more osteoclastogenesis than its parental LNCaP cells. These results demonstrated that the prostate cancer cell lines produce soluble factors that induce osteoclastogenesis. Because RANKL is a key osteoclastogenic factor that has been reported to exist in a soluble form (14–18), we next assessed if the prostate cancer cell lines' pro-osteoclastogenic activ-

ity could be blocked by OPG, a RANKL decoy receptor. The addition of OPG diminished the prostate cancer cell CM-induced osteoclastogenesis in a dose-dependent manner for both cell lines (Figure 1c). The ability of OPG to inhibit prostate cancer cell CM-induced osteoclastogenesis suggested that the prostate cancer cells induced osteoclastogenesis through sRANKL. However, these studies did not differentiate if the RANKL activity was derived directly from the prostate cancer cells or if the prostate cancer cells produced a soluble factor that induced RANKL from cells in the bone marrow stroma present in the murine bone marrow culture system. To differentiate between these possibilities, we tested the ability of C4-2B cell CM to induce osteoclastogenesis in a macrophage-like osteoclast precursor cell line, RAW 264.7, in the absence of supporting osteoblast/stromal cells. We found that exogenous (human recombinant) sRANKL itself can stimulate osteoclast formation in this in vitro culture system. Furthermore, CM from the C4-2B cells induced osteoclast formation that was inhibited by OPG in a dose-dependent manner. (Figure 2, a and b). These data provided strong evidence that the prostate cancer cells themselves produce active sRANKL. To confirm that possibility, we determined if the LNCaP and C4-2B cells expressed RANKL mRNA and protein. We found that both cell lines expressed RANKL mRNA (Figure 3a) and full-length RANKL protein (Figure 3b), as did the SaOS-positive control cell line. Finally, we detected sRANKL in concentrated CM from both LNCaP and C4-2B cells, but not SaOS cells (Figure 3b) at the molecular weight of 26 kDa as previously reported (14, 15). Taken together, these data provide evidence that prostate cancer cells are able to induce osteoclastogenesis directly through production of soluble RANKL.

The observation that OPG blocked C4-2B–induced osteoclastogenesis in vitro provided the rationale to test if OPG could prevent establishment of prostate cancer in bone in vivo. Accordingly, we evaluated the effect of OPG on the growth of C4-2B cells injected intratibially into SCID mice. Additionally, to determine if the effect was specific to bone, the same mice were inoculated with C4-2B cells subcutaneously at the time of intratibial tumor injection. Immediately after tumor cell injection, OPG (2 mg/kg) or vehicle was administered twice a week for 4 weeks through tail-vein injection. There were 15 mice per treatment group. One animal in the OPG treatment group died of unknown causes 1 day after the initial tumor injection. Four weeks after tumor injection, five mice from each group were sacrificed for evaluation. Skeletal lesions could not be identified by radiographs in either the vehicle or OPG-treated group (Table 1 and Figure 4); however, histological analysis revealed PSA-positive tumor infiltration in all the vehicle-treated animals, but not in any of the OPG-treated animals (Table 1 and Figure 4). Furthermore, there was an approximately eightfold increase of osteoclasts at the bone/tumor interface compared with the normal bone osteoclast perimeter observed in OPG-treated mice (Table 2). The osteoclast perimeter in the OPG-treated mice was similar to that in our previous report of osteoclast perimeter in untreated mice (12). The remaining mice were maintained for an additional 12 weeks at which time they

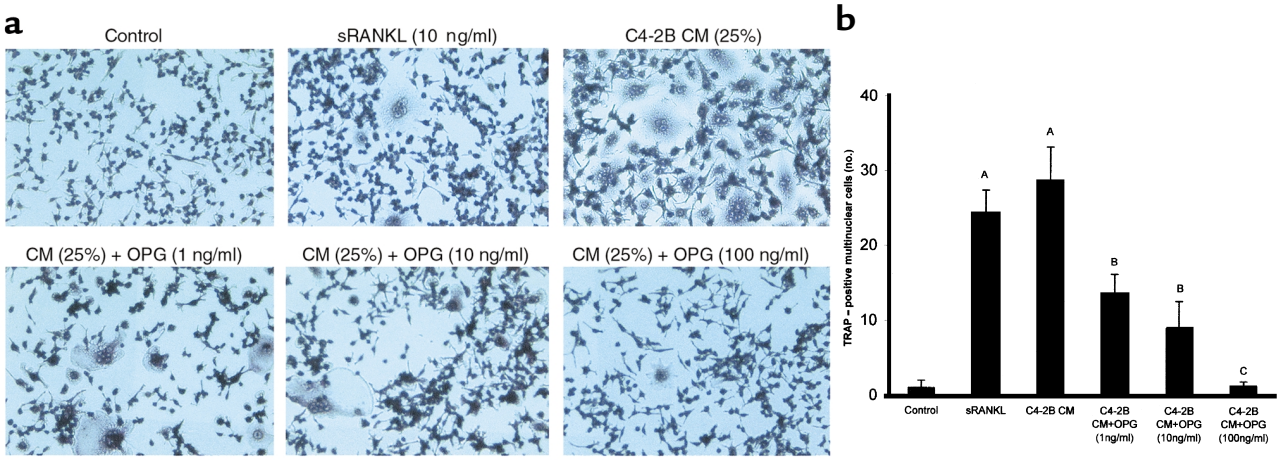

Figure 2

C4-2B CM induces osteoclastogenesis in the absence of osteoblast/stromal cells, and OPG inhibits the osteoclastogenesis in vitro. Single-cell suspensions (10^5 cells/well) of RAW 264.7 cells were plated in a 24-well plate on top of a sterile coverslip in RPMI plus 10% FBS. Cells were grown for 12 hours, then the media was changed to RPMI plus 0.5% FBS. CM from C4-2B cells was harvested (as described in Methods) and added to a final concentration of 25% (vol/vol). Immediately, recombinant human soluble RANKL (10 ng/ml) or the indicated concentration of recombinant mouse OPG or vehicle (1% BSA in PBS) was added. Osteoclasts were identified as TRAP-positive multinucleated (>3 nuclei) cells. (**a**) Representative pictures of cultures stained for TRAP. (**b**) Osteoclasts per coverslip were quantified. Samples were evaluated in quadruplicate. Results are reported as mean (±SD). Data were analyzed using one-way ANOVA. $^{A}P < 0.001$ compared with control culture; $^{B}P < 0.01$ compared with the CM-treated group; $^{C}P < 0.001$ compared with the CM-treated group.

Table 1
OPG prevents establishment of prostate cancer in the skeleton in mice

		4 weeks		16 weeks	
		Vehicle	OPG	Vehicle	OPG
Tibia	Radiologic	0/5	0/5	5/10	0/9[B]
	Histologic	5/5	0/5[A]	7/10	0/9[C]
Subcutis		4/5	5/5	10/10	8/9

Mice were injected intratibially and subcutaneously with C4-2B tumors, and then either vehicle or OPG (2 mg/kg) was administered intravenously twice a week for 4 weeks. The mice were sacrificed at the end of 4 weeks and 16 weeks after the initial injection of tumor. Tibial tumors were evaluated using radiography and histology. Subcutaneous tumors were evaluated by histology. The results are reported as the number of tumors for each group and total number of animals in each group. One mouse in the OPG-treatment died of unknown cause 1 day after the tumor injection, thus there were only nine animals in that group. [A]$P = 0.001$ compared with vehicle-treated animals; [B]$P = 0.03$ compared with vehicle-treated animals; [C]$P = 0.003$ compared with vehicle-treated animals. Data were analyzed by Fisher's exact test.

were sacrificed, and tumor burden was evaluated using radiography and histology. Tumor was not identified in lung, liver, spleen, brain, or vertebrae by histological evaluation. However, radiographs revealed marked osteolytic lesions with occasional foci of strongly osteoblastic lesions in the vehicle-treated animals compared with normal radiographs in the OPG-treated animals (Figure 4). Histology revealed that PSA-positive prostate cancer cells replaced the marrow in the vehicle-treated mice and a heterogeneous mixture of mostly shortened trabeculae with occasional areas consisting of thickened trabeculae (Figure 4). These data confirmed that the PSA-positive C4-2B tumor cells were growing in the vehicle-treated mice. Furthermore, the absence of PSA-positive cells in the OPG-treated mice supports that there was either no or a minimal tumor burden in these mice. Finally, we observed a high number of TRAP-positive osteoclasts at the bone/tumor interface (Figure 5), indicating that mature osteoclasts were directly adjacent to tumor with increased activity. Histomorphometric quantification of osteoclast number at the bone/tumor interface revealed an approximately 15-fold increase of osteoclasts in the vehicle-treated animals compared with normal bone surface in the OPG-treated animals (Table 2). Taken together, these data demonstrate that OPG inhibits the development of C4-2B–derived tumors, including both osteolytic and osteoblastic components. Furthermore, the data strongly suggest that the development of osteoblastic lesions is dependent on osteoclastic activity.

The incidence of tumor growth in the bone at 16 weeks after tumor injection in the vehicle-treated mice was 50% and 70%, based on radiography and histology, respectively (Table 1). In contrast, intratibial tumor was not detected by radiography or histology in the OPG-treated mice (Table 1). Furthermore, in contrast to tumor growth at the bone site, there was no difference in subcutaneous tumor incidence between vehicle-treated and OPG-treated mice (Table 1), and the growth rate of the subcutaneous tumors did not differ between the groups (Figure 6). Taken together, these data demonstrate that OPG preferentially inhibits C4-2B tumor growth in bone. The data also suggest that OPG does not have a direct effect on tumor growth, as the subcutaneous tumors grew similarly in the vehicle-treated and OPG-treated groups. This is further supported by the observation that OPG had no effect on proliferation, cell viability, and basal apoptotic rate of C4-2B cells in vitro (data not shown; experimental protocols were described in Methods).

Discussion

In 1958, Roland introduced the theory that every primary or metastatic cancer in bone (including osteoblastic prostate cancers) begins with osteolysis (19). However, while important gains in understanding the role of osteoclastic activity have been made for osteolytic tumors, the importance of osteoclastic activity in the development of prostate cancer skeletal metastatic lesions has received little attention because of their overall osteoblastic radiographic appearance. Yet, despite the radiographic appearance, it is clear from histological evidence that prostate cancer metastases form a heterogeneous mixture of osteolytic and osteoblastic lesions (2, 20–23). In fact, histomorphometric analysis of metastatic lesions reveals that osteoblastic metastases form on trabecular bone at sites of previous osteoclastic resorption, suggesting that bone resorption is required for subsequent osteoblastic bone formation (2). To test this hypothesis, we determined if inhibiting osteoclastogenesis would prevent establishment of a prostate cancer

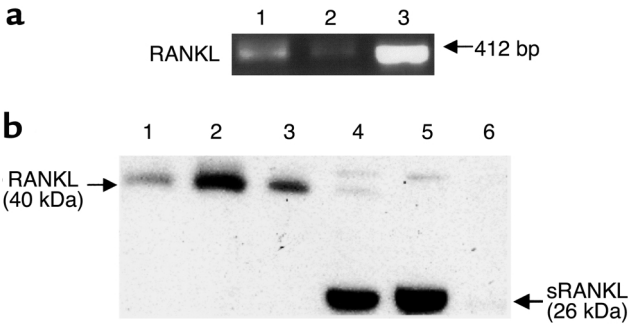

Figure 3
LNCaP and C4-2B cells express RANKL and produce soluble RANKL. (**a**) One microgram of total RNA from the indicated cells was subjected to RT-PCR. Lanes 1, 2, and 3 are PCR products from LNCaP, C4-2B, and SaOS, respectively. (**b**) Total cellular protein or CM (concentrated 100-fold using Microcon centrifugal filter devices) from LNCaP, C4-2B, and SaOS cell cultures were subjected to Western blot analysis (50 μg/lane) using rabbit anti-human soluble RANKL polyclonal Ab as primary Ab and HRP-conjugated anti-rabbit IgG as secondary Ab. Bands were detected using luminescence and autoradiography. Lane 1, LNCaP cell lysate; lane 2, C4-2B cell lysate; lane 3, SaOS cell lysate; lane 4, LNCaP concentrated CM; lane 5, C4-2B concentrated CM; and lane 6, SaOS concentrated CM.

Table 2
Histomorphometric quantification of OC perimeter at bone/tumor interface in the vehicle-treated mice compared with normal bone surface in the OPG-treated mice

	4 weeks		16 weeks	
	Vehicle	OPG	Vehicle	OPG
OC perimeter (no. OC/mm)	10.84 ± 2.60	1.40 ± 0.46[A]	20.02 ± 3.68	1.36 ± 0.63[B]

[A]$P < 0.01$ compared with vehicle-treated animals; [B]$P < 0.001$ compared with vehicle-treated animals. Student's *t* test.

xenograft, which forms mixed osteoblastic and osteoclastic lesions, in the tibia of mice. The results from the present study demonstrate that prostate cancer cells can directly induce osteoclastogenesis through production of sRANKL. Additionally, this study demonstrates that OPG-mediated inhibition of osteoclastogenesis was associated with prevention of C4-2B cell growth in osseous, but not in nonosseous tissue. Finally, the observation that OPG did not diminish subcutaneous growth of the tumor, in combination with the observation that OPG had no direct affect on the prostate cancer cells in vitro suggests that OPG's ability to inhibit prostate cancer establishment was due specifically to factors in the bone microenvironment. These data suggest that inhibition of osteoclast activity is sufficient to diminish the development of skeletal metastatic prostate tumors that have both osteolytic and osteoblastic components.

Our results are consistent with reports that most prostate cancer skeletal metastasis reveals an osteoclastic component (2–4). Based on the data in this report, together with earlier evidence that tumors that metastasize to bone require osteoclastic activity to release tumor-supportive growth factors from bone (reviewed in ref. 24), it appears that osteoclastogenesis is an important mediator of prostate cancer establishment in the bone in this murine model. These results are reflected in clinical data, which demonstrate that systemic markers of bone resorption are increased in men with prostate cancer skeletal metastases (25, 26) and that bisphosphonates relieve bone pain in this population of patients (27, 28). In the case of bisphosphonates, however, it is unknown if this effect is due to inhibiting osteoclastic activity or due to a direct tumor effect (29, 30).

The C4-2B prostate cancer cells have been reported previously to induce marked osteoblastic skeletal lesions (8, 9). In the current study, we observed osteoblastic areas on radiographs and histology; however, osteolytic lesions were predominant. We cannot readily account for

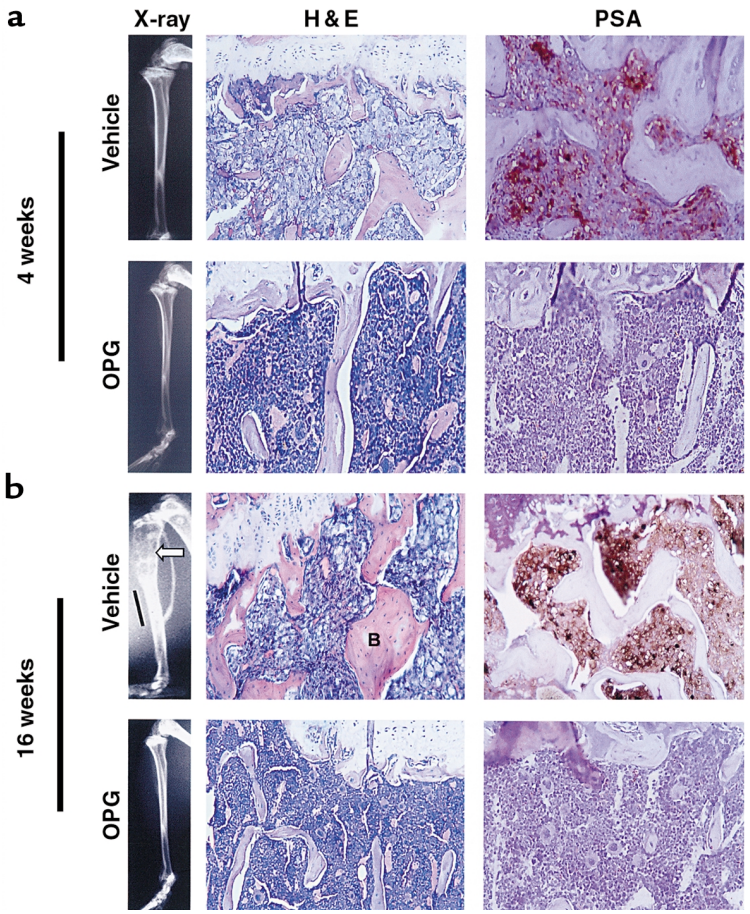

Figure 4
Characteristics of C4-2B bone lesions. SCID mice were injected intratibially with C4-2B prostate cancer cells. At the time of tumor injection, OPG (2 mg/kg) or vehicle (1% BSA in 1× PBS) was administered via the tail vein twice a week for 4 weeks. The mice were sacrificed at 4 weeks and 16 weeks after-tumor injection. Formalin-fixed paraffin-embedded sections were stained with hematoxylin and eosin (H&E) or were deparaffinized, rehydrated, and stained for PSA using immunohistochemistry. Brown coloration indicates presence of PSA. ×200. (**a**) Representative radiographs of H&E- and PSA-stained sections of vehicle-treated versus OPG-treated mice at the end of 4 weeks. Note replacement of bone marrow by tumor in the vehicle-treated animals compared with normal marrow in OPG-treated animals. PSA staining cannot be identified in the OPG-treated animals. (**b**) Representative radiographs of H&E- and PSA-stained sections of vehicle-treated versus OPG-treated mice at the end of 16 weeks. Note the area of osteolysis (arrowhead) and osteoblastic lesion (bar) in the radiograph of the vehicle-treated mouse compared with the normal radiograph of the OPG-treated mice. Also, note the replacement of bone marrow by tumor and the thickened trabeculum indicated with letter B in the vehicle-treated mouse compared with the OPG-treated mouse.

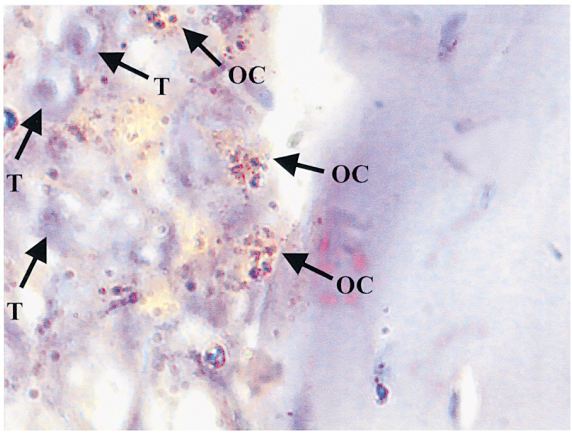

Figure 5
C4-2B cells promote osteoclast activity at bone/tumor interface. SCID mice were injected intratibially with C4-2B prostate cancer cells. Tibias were harvested 16 weeks after tumor injection, decalcified, sectioned, and stained for TRAP. A section is shown that demonstrates multiple TRAP-positive staining osteoclasts at the bone/tumor interface. T, tumor cell; OC, multinucleated TRAP-positive osteoclast. ×1000 under oil.

the discrepancy with previous reports. However, in those studies, tumors were observed in femur, vertebrae, or pelvis (31), in contrast to tibia, as in the current study. Thus, one possibility to account for different degrees of osteoblastic response is the difference in bone remodeling that occurs at different skeletal regions (32–34).

Our observations that C4-2B CM induced osteoclastogenesis from RAW 244.7 cells in the absence of supporting stroma or M-CSF strongly suggested that the CM contained RANKL activity (35). This was further confirmed by the observations that OPG diminished prostate cancer cell CM-induced osteoclastogenesis in RAW 264.7 cells in the absence of supporting marrow stroma and that the CM contained sRANKL. These results suggest that prostate cancer cells directly contribute to osteolysis in vivo through induction of osteoclastogenesis at the metastatic tumor sites and are consistent with reports of the presence of sRANKL in several other cancer cell lines and activated T cells (14–18). In these reports, sRANKL was produced through either proteolytic cleavage of the extracellular portion of RANKL (15, 16) or from an mRNA that encoded a secreted form of RANKL (17). Thus, it is plausible that prostate cancer cells, through their production of proteolytic enzymes such as PSA or metalloproteases (36, 37), cleave the extracellular domain of RANKL, resulting in sRANKL production. Furthermore, the low levels of metalloproteases in SaOS cells may account for our inability to detect sRANKL in the SaOS CM (38).

Our observation that prostate cancer cells express RANKL and directly induce osteoclastogenesis contrasts with reports that an osteolytic murine melanoma and several human breast cancer cell lines do not express RANKL (39, 40). In terms of the murine melanoma cells, RANKL expression was induced in cocultures of melanoma and bone marrow cells (40). However, the source of RANKL was not identified in that study. In contrast, breast cancer cells indirectly induced osteoclastogenesis through upregulation of RANKL in bone marrow stroma and osteoblasts (39). Thus, our results provide a novel mechanism through which discrete osteolytic bone lesions are produced directly by tumor cell–derived sRANKL. This finding is in agreement with the recent report of an mRNA encoding a sRANKL in squamous cell carcinoma cell lines derived from parental malignant tissues that was associated with severe humoral hypercalcemia (17). It is not clear why prostate cancer cell lines express RANKL and breast cancer cell lines do not. One possible explanation accounting for this difference is that as prostate cancer cells progress to a skeletal metastatic phenotype, they take on osteoblast-like characteristics, including production of osteoblast proteins such as bone sialoprotein and osteonectin, expression of the osteoblast-specific transcription factor, Cbfa1, and the ability to form hydroxyapatite in vitro (41, 42). It follows that expression of RANKL, which is expressed in osteoblast, may be upregulated as part of this general phenomenon.

The observation that OPG–mediated prevention of intratibial tumor growth was associated with diminished osteoclastogenesis in vivo, as determined by bone histomorphometry, is consistent with the hypothesis that osteoclast activity is required for establishment of the prostate cancer in bone. In addition to inhibiting osteoclastogenesis, it is possible that OPG directly impaired prostate tumor growth in parallel with its antiosteoclastogenic effect. For example, RANKL is required to prevent apoptosis of epithelial mammary cells through interaction with RANK on the mammary cell surface

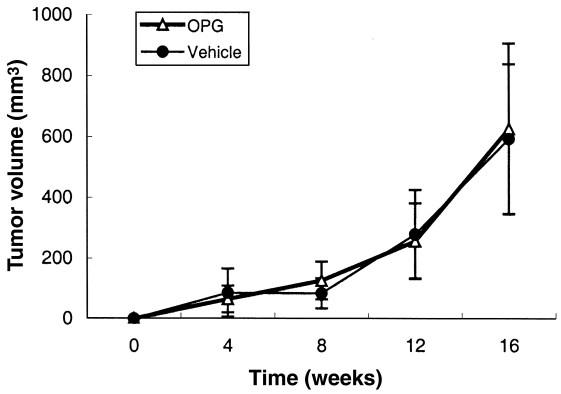

Figure 6
OPG does not affect subcutaneous tumor growth in mice. C4-2B prostate cancer cells were injected subcutaneously into the SCID mice at the same time they received intratibial tumor injection as described in Figure 4. At the time of tumor injection, OPG (2 mg/kg) or vehicle (1% BSA in 1× PBS) was administered via the tail vein twice a week for 4 weeks. Tumors were allowed to grow for another 12 weeks. The mice were sacrificed at 16 weeks after tumor injection. Tumor volume was measured monthly. Data are reported as mean (±SD) from nine to ten animals per group.

during development (43). This observation raises the possibility that OPG, which blocks RANKL activity, may induce apoptosis of other epithelial cell types, including prostate cells. However, based on the observations that (1) direct administration of OPG had no detectable effect on prostate cancer cell proliferation, viability or apoptotic rate in vitro and (2) OPG did not impair prostate tumor growth in the subcutaneous site, it is unlikely that OPG mediated its tumor growth preventative effects through a similar mechanism. Taken together, these data provide support to the possibility that OPG prevents prostate tumor establishment in bone through inhibition of osteoclastogenesis in this animal model. However, the current experiments do not completely rule out that OPG enhanced the expression of factors that inhibit tumor growth specifically in the bone microenvironment.

Our result that OPG prevented both osteolysis and establishment of tumor is in agreement with a previous report that LNCaP cells implanted in the femurs of nude mice initially formed tumor in bone, which spontaneously regressed to be replaced by normal marrow (44). However, our results present an interesting contrast to several studies that have examined the effect of inhibiting osteoclastic activity on tumor development in mice. In one study, ibandronate prevented myeloma-associated osteoclastogenesis (45), and in another study OPG diminished the osteolytic component of a primary sarcoma implanted in the bone of mice (7); but in contrast to our study, tumor volume was not decreased compared with control animals in either study. Possible reasons for this difference between the current study and these previous reports may be because bone was the myeloma's and sarcoma's primary site, thus the tumor was in a favorable environment and may readily thrive in the bone microenvironment. In contrast, prostate cancer is an epithelial tissue derived from a site other than bone, and thus the prostate cells are in a "hostile" environment as proposed previously (41). Furthermore, it has been suggested that the bone resorption releases growth factors from the bone matrix that promote tumor growth (24). Thus, the prostate cancer cells may not thrive in the hostile bone microenvironment in the presence of osteoclast activity and the resulting release of growth factors.

In summary, results from the current study demonstrated that prostate cancer cells produce sRANKL and induce osteoclastogenesis in vitro. Furthermore, it demonstrated that OPG prevents establishment of prostate cancer in bone, but not in subcutaneous tissue. Taken together, these results suggest the osteoclast activity is an important component of the establishment of prostate cancer in the skeleton and that inhibition of osteoclastic activity may prevent establishment or slow progression of skeletal metastatic lesions, including those with an osteoblastic component.

Acknowledgments

We would like to thank Robert Vessella and his laboratory for sharing the intratibial injection technique and Julie Brown for sharing RANKL primer sequences with us. We would like to thank Zhiming Huang for reviewing slides of bone pathology. This work was supported by US Army Medical Research Material Command Prostate Cancer Research Program grant DAMD17-00-1-053 and the NIH grants R01 AG-15904, P50 CA-69568, and T32 RR-07008.

1. Abrams, H., Spiro, R., and Goldstein, N. 1950. Metastases in carcinoma. *Cancer.* **3**:74–85.
2. Charhon, S.A., et al. 1983. Histomorphometric analysis of sclerotic bone metastases from prostatic carcinoma special reference to osteomalacia. *Cancer.* **51**:918–924.
3. Urwin, G.H., et al. 1985. Generalised increase in bone resorption in carcinoma of the prostate. *Br. J. Urol.* **57**:721–723.
4. Clarke, N.W., McClure, J., and George, N.J. 1992. Disodium pamidronate identifies differential osteoclastic bone resorption in metastatic prostate cancer. *Br. J. Urol.* **69**:64–70.
5. Clarke, N. 1998. The effects of pamidronate disodium treatment in metastatic prostate cancer. *Rev. Contemp. Pharamcother.* **9**:205–212.
6. Teitelbaum, S.L. 2000. Bone resorption by osteoclasts. *Science.* **289**:1504–1508.
7. Honore, P., et al. 2000. Osteoprotegerin blocks bone cancer-induced skeletal destruction, skeletal pain and pain-related neurochemical reorganization of the spinal cord. *Nat. Med.* **6**:521–528.
8. Wu, T.T., et al. 1998. Establishing human prostate cancer cell xenografts in bone: induction of osteoblastic reaction by prostate-specific antigen-producing tumors in athymic and SCID/bg mice using LNCaP and lineage-derived metastatic sublines. *Int. J. Cancer.* **77**:887–894.
9. Thalmann, G.N., et al. 1994. Androgen-independent cancer progression and bone metastasis in the LNCaP model of human prostate cancer. *Cancer Res.* **54**:2577–2581.
10. Berlin, O., et al. 1993. Development of a novel spontaneous metastasis model of human osteosarcoma transplanted orthotopically into bone of athymic mice. *Cancer Res.* **53**:4890–4895.
11. Davol, P.A., and Frackelton, A.R., Jr. 1999. Targeting human prostatic carcinoma through basic fibroblast growth factor receptors in an animal model: characterizing and circumventing mechanisms of tumor resistance. *Prostate.* **40**:178–191.
12. Dai, J., et al. 2000. Chronic alcohol ingestion induces osteoclastogenesis and bone loss through IL-6 in mice. *J. Clin. Invest.* **106**:887–895.
13. Heymann, D., Guicheux, J., Gouin, F., Passuti, N., and Daculsi, G. 1998. Cytokines, growth factors and osteoclasts. *Cytokine.* **10**:155–168.
14. Lacey, D.L., et al. 1998. Osteoprotegerin ligand is a cytokine that regulates osteoclast differentiation and activation. *Cell.* **93**:165–176.
15. Lum, L., et al. 1999. Evidence for a role of a tumor necrosis factor-alpha (TNF-alpha)-converting enzyme-like protease in shedding of TRANCE, a TNF family member involved in osteoclastogenesis and dendritic cell survival. *J. Biol. Chem.* **274**:13613–13618.
16. Nakashima, T., et al. 2000. Protein expression and functional difference of membrane-bound and soluble receptor activator of NF-kappaB ligand: modulation of the expression by osteotropic factors and cytokines. *Biochem. Biophys. Res. Commun.* **275**:768–775.
17. Nagai, M., Kyakumoto, S., and Sato, N. 2000. Cancer cells responsible for humoral hypercalcemia express mRNA encoding a secreted form of ODF/TRANCE that induces osteoclast formation. *Biochem. Biophys. Res. Commun.* **269**:532–536.
18. Weitzmann, M.N., Cenci, S., Rifas, L., Brown, C., and Pacifici, R. 2000. Interleukin-7 stimulates osteoclast formation by up-regulating the T-cell production of soluble osteoclastogenic cytokines. *Blood.* **96**:1873–1878.
19. Roland, S. 1958. Calcium studies in ten cases of osteoblastic prostatic metastasis. *J. Urol.* **79**:339–342.
20. Berruti, A., et al. 1996. Biochemical evaluation of bone turnover in cancer patients with bone metastases: relationship with radiograph appearances and disease extension. *Br. J. Cancer.* **73**:1581–1587.
21. Vinholes, J., Coleman, R., and Eastell, R. 1996. Effects of bone metastases on bone metabolism: implications for diagnosis, imaging and assessment of response to cancer treatment. *Cancer Treat. Rev.* **22**:289–331.
22. Nemoto, R., Kanoh, S., Koiso, K., and Harada, M. 1988. Establishment of a model to evaluate inhibition of bone resorption induced by human prostate cancer cells in nude mice. *J. Urol.* **140**:875–879.
23. Roudier, M., et al. 2000. Heterogenous bone histomorphometric patterns in metastatic prostate cancer. *J. Bone Miner. Res.* **15S1**:S567. (Abstr.)
24. Guise, T.A. 2000. Molecular mechanisms of osteolytic bone metastases. *Cancer.* **88**:2892–2898.

25. Garnero, P., et al. 2000. Markers of bone turnover for the management of patients with bone metastases from prostate cancer. *Br. J. Cancer.* **82**:858–864.
26. Fontana, A., and Delmas, P.D. 2000. Markers of bone turnover in bone metastases. *Cancer.* **88**:2952–2960.
27. Pelger, R.C., et al. 1998. Effects of the bisphosphonate olpadronate in patients with carcinoma of the prostate metastatic to the skeleton. *Bone.* **22**:403–408.
28. Heidenreich, A., Hofmann, R., and Engelmann, U.H. 2001. The use of bisphosphonate for the palliative treatment of painful bone metastasis due to hormone refractory prostate cancer. *J. Urol.* **165**:136–140.
29. Coleman, R.E. 2000. Optimising treatment of bone metastases by arediatm and zometatm. *Breast Cancer.* **7**:361–369.
30. Boissier, S., et al. 2000. Bisphosphonates inhibit breast and prostate carcinoma cell invasion, an early event in the formation of bone metastases. *Cancer Res.* **60**:2949–2954.
31. Thalmann, G.N.N., et al. 2000. LNCaP progression model of human prostate cancer: androgen-independence and osseous metastasis. *Prostate.* **44**:91–103.
32. Verna, C., Melsen, B., and Melsen, F. 1999. Differences in static cortical bone remodeling parameters in human mandible and iliac crest. *Bone.* **25**:577–583.
33. Chiodini, I., et al. 1998. Alterations of bone turnover and bone mass at different skeletal sites due to pure glucocorticoid excess: study in eumenorrheic patients with Cushing's syndrome. *J. Clin. Endocrinol. Metab.* **83**:1863–1867.
34. Carnevale, V., et al. 2000. Different patterns of global and regional skeletal uptake of 99mTc-methylene diphosphonate with age: relevance to the pathogenesis of bone loss. *J. Nucl. Med.* **41**:1478–1483.
35. Hsu, H., et al. 1999. Tumor necrosis factor receptor family member RANK mediates osteoclast differentiation and activation induced by osteoprotegerin ligand. *Proc. Natl. Acad. Sci. USA.* **96**:3540–3545.
36. Lein, M., et al. 1999. Metalloproteinases and tissue inhibitors of matrix-metalloproteinases in plasma of patients with prostate cancer and in prostate cancer tissue. *Ann. NY Acad. Sci.* **878**:544–546.
37. Nagakawa, O., et al. 2000. Expression of membrane-type 1 matrix metalloproteinase (MT1-MMP) on prostate cancer cell lines. *Cancer Lett.* **155**:173–179.
38. Rifas, L., Fausto, A., Scott, M.J., Avioli, L.V., and Welgus, H.G. 1994. Expression of metalloproteinases and tissue inhibitors of metalloproteinases in human osteoblast-like cells: differentiation is associated with repression of metalloproteinase biosynthesis. *Endocrinology.* **134**:213–221.
39. Thomas, R.J., et al. 1999. Breast cancer cells interact with osteoblasts to support osteoclast formation. *Endocrinology.* **140**:4451–4458.
40. Chikatsu, N., et al. 2000. Interactions between cancer and bone marrow cells induce osteoclast differentiation factor expression and osteoclast-like cell formation in vitro. *Biochem. Biophys. Res. Commun.* **267**:632–637.
41. Koeneman, K.S., Yeung, F., and Chung L.W. 1999. Osteomimetic properties of prostate cancer cells: a hypothesis supporting the predilection of prostate cancer metastasis and growth in the bone environment. *Prostate.* **39**:246–261.
42. Lin, D., et al. 2001. The bone metastatic LNCaP-derivative C4-2B prostate cancer cell line induces mineralization in vitro. *Prostate.* In press.
43. Fata, J.E., et al. 2000. The osteoclast differentiation factor osteoprotegerin-ligand is essential for mammary gland development. *Cell.* **103**:41–50.
44. Soos, G., Jones, R.F., Haas, G.P., and Wang, C.Y. 1997. Comparative intraosseal growth of human prostate cancer cell lines LNCaP and PC-3 in the nude mouse. *Anticancer Res.* **17**:4253–4258.
45. Dallas, S.L., et al. 1999. Ibandronate reduces osteolytic lesions but not tumor burden in a murine model of myeloma bone disease. *Blood.* **93**:1697–1706.